BN-Heterocycles

International Edition: DOI: 10.1002/anie.201507770
German Edition: DOI: 10.1002/ange.201507770

In Situ Solid-State Generation of $(BN)_2$-Pyrenes and Electroluminescent Devices

Suning Wang, Deng-Tao Yang, Jiasheng Lu, Hiroyuki Shimogawa, Shaolong Gong,* Xiang Wang, Soren K. Mellerup, Atsushi Wakamiya, Yi-Lu Chang, Chuluo Yang, and Zheng-Hong Lu**

Abstract: *New BN-heterocyclic compounds have been found to undergo double arene photoelimination, forming rare yellow fluorescent BN-pyrenes that contain two B–N units. Most significant is the discovery that the double arene elimination can also be driven by excitons generated electrically within electroluminescent (EL) devices, enabling the in situ solid-state conversion of BN-heterocycles to BN-pyrenes and the use of BN-pyrenes as emitters for EL devices. The in situ exciton-driven elimination (EDE) phenomenon has also been observed for other BN-heterocycles.*

BN-arenes are a special class of π-conjugated materials, in which pairs of carbon atoms are replaced by a B–N unit.[1] Following the pioneering work of Dewar and co-workers more than 50 years ago,[2] many entries in this class of compounds have been shown to display unique photophysical and/or electronic properties implying a number of potential uses as optoelectronic materials.[3–6] In fact, several BN-arenes have been shown to be highly effective and often superior, compared to their all carbon analogues, as components in devices such as organic field-effect transistors (OFETs).[5] These recent findings have inspired intense research efforts in the development of new synthetic methodologies for BN-arenes, leading to an increasing number of diverse examples appearing throughout the literature.[1–8] Despite these successes, however, the practical implementation of such species has proved to be quite challenging owing to various issues associated with extended π-conjugated materials such as stability and processability. Furthermore, many interesting and rare BN-arene compounds are not accessible by conventional synthetic approaches.

For example, BN-pyrenes are attractive target molecules because of their extended conjugated structure as well as the highly fluorescent nature of pyrene analogues.[9] However, only three examples of BN-pyrenes have been reported to date, namely **(BN)-pyrene-1**,[2e] **(BN)-pyrene-2**,[6] and **$(BN)_2$-pyrene-1**[2a,7] (Figure 1), of which only **(BN)-pyrene-2** and its derivatives were shown to be fluorescent.[6] Computational data of the analogues shown in Figure 1 suggests that the location and number of B–N units within the pyrene skeleton dramatically affects the electronic structure of these molecules, and consequently, their photophysical properties as well. Among the BN-pyrenes described above, **$(BN)_2$-pyrene-2** and **$(BN)_2$-pyrene-3** are most interesting as they possess small HOMO–LUMO gaps and stabilized LUMO levels according to the DFT data (see the Supporting Information for details). However, these two compounds are not accessible by common synthetic methods.

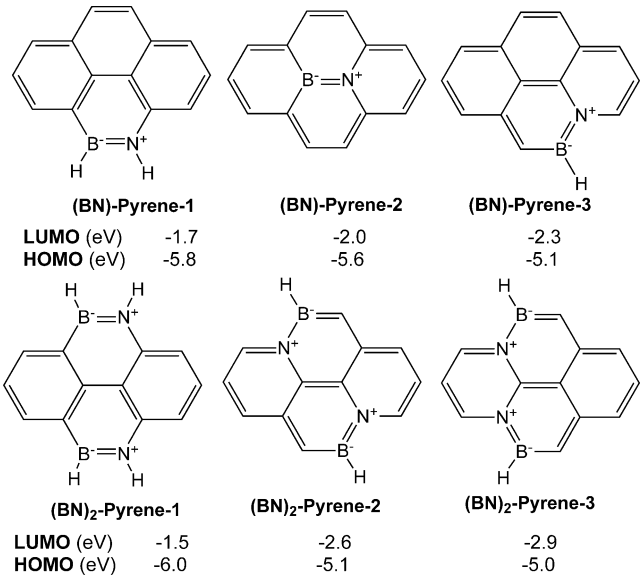

Figure 1. DFT calculated HOMO–LUMO energy levels of selected BN-pyrenes.

[*] Prof. Dr. S. Wang
Beijing Key Laboratory of Photoelectronic/Electrophotonic Conversion Materials
School of Chemistry, Beijing Institute of Technology
Beijing 100081 (P.R. China)
E-mail: sw17@queensu.ca
wangsn14@bit.edu.cn
Prof. Dr. S. Wang, D.-T. Yang, J. Lu, X. Wang, S. K. Mellerup
Department of Chemistry, Queen's University
Kingston, Ontario K7L 3N6 (Canada)
Prof. Dr. S. Gong, Dr. Y.-L. Chang, Prof. Dr. Z.-H. Lu
Department of Materials Sciences and Engineering
University of Toronto
184 College Street, Toronto, Ontario M5S 3E4 (Canada)
E-mail: shaolong.gong@utoronto.ca
zhenghong.lu@utoronto.ca
H. Shimogawa, Prof. Dr. A. Wakamiya
Institute for Chemical Research, Kyoto University
Uji, Kyoto 611-0011 (Japan)
Prof. Dr. S. Gong, Prof. Dr. C. Yang
Hubei Key Lab on Organic and Polymeric Optoelectronic Materials
Department of Chemistry, Wuhan University
Wuhan 430072 (China)

Supporting information for this article is available on the WWW under http://dx.doi.org/10.1002/anie.201507770.

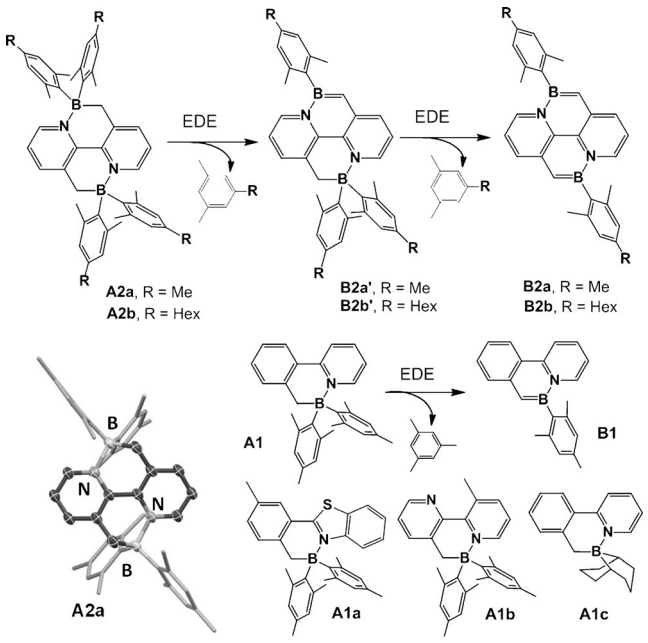

Figure 2. The EDE reactions of **A1**, **A2a**, and **A2b**, the crystal structure of **A2a**, and the structures of **A1a**–**A1c**.

Based on our recent successful synthesis of a number of BN-phenanthrenes (**B1** in Figure 2 and derivatives) via photolytic or thermal elimination reactions[8] of benzyl-pyridyl BR_2 chelate compounds (BN-heterocycles, for example, **A1**), we envisioned that it may be possible to obtain **(BN)$_2$pyrene-2** and **(BN)$_2$pyrene-3** and their derivatives by a similar approach. Hence, we addressed the synthesis of the BN-heterocyclic precursor molecules for these two compounds. Although our attempts to synthesize the precursor compound for the **(BN)$_2$pyrene-3** derivatives failed, the precursors for **(BN)$_2$pyrene-2** derivatives (**A2a** and **A2b**) were successfully obtained. During the investigation of the elimination reactions of **A2a** and **A2b**, we discovered that these precursor molecules could also be converted to the corresponding bis(BN-pyrenes) through the use of excitons generated electrically inside an electroluminescent (EL) device, as shown in Figure 2. We have further established that this unprecedented in situ exciton-driven elimination reaction (EDE) in a solid-state device is a general process and can be applied to other BN-heterocycles such as **A1**, **A1a**, and **A1b** (Figure 2). This discovery unveils a new property/utility of BN-heterocycles and also provides an innovative design strategy for both the fabrication of optoelectronic devices based on BN-arenes and the incorporation of such conjugated materials within said devices. The details are presented herein.

Precursors **A1** and **A1a**–**A1c** were synthesized according to previously reported procedures.[8] Molecules **A2a** and **A2b** were prepared via double lithiation of 3,3′-dimethyl-2,2′bipyridine,[10] followed by the addition of two equivalents of the appropriate BAr_2F reagent. The bulky aryl groups on the boron center were chosen to enhance the chemical stability and reduce excimer emission of the BN-pyrenes, as well as ensure high thermal stability of the precursors. Compounds **A2a** and **A2b** were fully characterized by NMR spectroscopy and HRMS. The crystal structure of **A2a** was determined by X-ray diffraction analysis and is shown in Figure 2. **A2a** is thermally stable up to roughly 284 °C (melting point (m.p.)/decomposition temperature see Figure S6 in the Supporting Information), while **A2b** has a low melting point at 184 °C. Both **A2a** and **A2b** have a strong absorption band at $\lambda_{max} \approx 350$ nm and are weakly emissive in the UV region with $\lambda_{em} \approx 380$ nm in THF.

Upon irradiation at 350 nm, the light yellow solution of **A2a** or **A2b** gradually becomes red–orange with a new absorption band appearing in the 400–600 nm region, which is attributed to the BN-pyrene species **B2a/B2b**. HRMS analysis (see Figure S1) confirmed the formation of both single-elimination (**B2a′**) and double-elimination products (**B2a**) from the photoreaction shown in Figure 2. However, the fluorescence of **B2a′/B2b′** was not detected. **B2a** could not be characterized by NMR spectroscopy because it is insoluble in common NMR solvents. Due to the solubility-enhancing hexyl groups in **A2b**, it was possible to monitor the double-photoelimination process by ^{1}H NMR spectroscopy, which established unequivocally the clean transformation of **A2b** to **B2b** over a period of several days at the typical NMR concentration scale (see Figure S2). Interestingly, the single-elimination product **B2b′** was not observed in the NMR spectra, indicating that it may be short-lived and transforms readily to **B2b** upon its formation in solution. Compared to **A1**, the photoelimination of **A2a** and **A2b** are much slower and less efficient under the same conditions, which is likely caused by their highly congested structures (see the crystal structure of **A2a**), leading to an unstable transition state[8b,c] in the reaction pathway toward **B2a′/B2b′**.

To further understand the elimination reaction of **A2a** and **A2b**, DFT computations on the elimination pathways of **A2a** were performed, and the results indicate that the stepwise elimination shown in Figure 2 is the only energetically favorable pathway (see Figure S7b for details). The calculated thermal activation barriers for the first and second elimination steps are in fact similar. The seemingly rapid conversion of **B2a′/B2b′** to **B2a/B2b** may be facilitated by the enhanced conjugation of **B2a′/B2b′**, compared to **A2a/A2b** that stabilizes the transition state in the excited state.

Both **B2a** and **B2b** display bright yellow fluorescence in solution and in the solid state ($\lambda_{max} \approx 570$ nm, Figure 3) and their fluorescent spectra have well-resolved vibrational features. The fluorescence quantum efficiency of **B2b** was determined to be 0.27 in THF (using $[Ir(ppy)_3]$ as the reference[11]). Interestingly, the absorption and fluorescent peaks of **B2a** and **B2b** have very small Stokes shifts (ca. 10 nm) as shown in Figure 3, which is clearly due to their rigid structure and the symmetry-allowed $S_0 \rightarrow S_1$ transitions in these BN-pyrenes. In contrast to pyrene which is highly prone to excimer emission,[10] **B2a** and **B2b** do not display excimer emission, which is credited to the bulky aryl group on each boron atom. Compared to the green-emissive BN-phenanthrene **B1** which has an emission peak at around 495 nm,[8a] the maxima of the absorption and fluorescent bands of **B2a** and **B2b** are red-shifted by ca. 70 nm, which is consistent with the greater π-conjugation in **B2a** and **B2b**. TD-DFT compu-

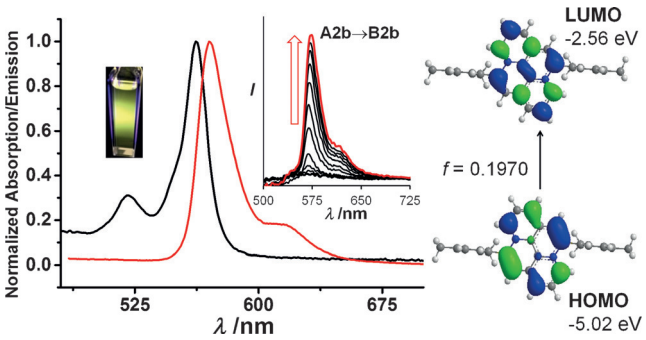

Figure 3. Left: The absorption (black) and fluorescence (red) spectra of **B2b** in THF. Inset: a photograph showing the emission color of **B2b** in THF and the change in the fluorescence spectrum of **A2b** in a PMMA film (20 wt%) with 350 nm irradiation. Right: The MO diagrams of **B2a** involved in the $S_0 \rightarrow S_1$ transition.

tational studies (see the Supporting Information) confirmed that the $S_0 \rightarrow S_1$ transitions of **B2a** and **B2b** involve primarily the HOMO and LUMO orbitals (97%), which are localized on the BN-pyrene ring with a very high oscillator strength (0.1970, Figure 3) and believed to be responsible for the yellow fluorescence of these molecules. The optical energy gap (ca. 2.06 eV) of **B2a** and **B2b** is about 1.5 eV smaller than that of pyrene. Compared to the previously reported **(BN)-pyrene-2** and its derivatives,[6] the absorption band of **B2a**/**B2b** is red-shifted by about 120 nm while the fluorescent band is red-shifted by approximately 70–90 nm, which is consistent with the general trend predicted by DFT data. **B2b** displays a reversible one-electron reduction in THF at −2.10 V, a potential about 0.40 V more positive than that of **B1**, and an irreversible oxidation at 0.35 V (vs. $[FeCp_2]^+/[FeCp_2]$), corresponding to approximate HOMO and LUMO levels of −5.15 and −2.70 eV, respectively. These properties make **B2a** and **B2b** promising candidates for use as yellow emitters in EL devices.

Due to the slow, inefficient photoelimination of **A2a/A2b** and air-sensitive nature of **B2a/B2b**, it is difficult to synthesize large quantities of the BN-pyrenes for applications in EL devices using the photochemical procedure. We therefore postulated that perhaps the precursor species **A2a**/**A2b** could be directly converted to **B2a**/**B2b** using excitons within the EL devices, namely, the aforementioned in situ EDE procedure. Since EL devices employ materials in the solid state, it was necessary to first establish that the double photoelimination of **A2a**/**A2b** can occur in the condensed phase. Indeed, we found that compounds **A2a** and **A2b** underwent double photoelimination in PMMA films (20 wt%), forming **B2a** and **B2b** as evidenced by the fluorescence spectra shown in Figure 3. Next, an EL device incorporating **A2a** was fabricated using vacuum deposition. To demonstrate the generality of the EDE method, EL devices incorporating compounds **A1** and **A1a**–**A1c** were also fabricated. **A2b** is not suitable for EL device fabrication via vacuum deposition because of its high molecular weight and relatively low melting point.

The details of the EL work based on **A1** and **A2a** are presented here. The device data for other compounds are provided in Figure S8b–j. A standard EL device structure was adopted (Figure 4a) for all compounds in which MoO_3 and LiF serve as hole- and electron-injection layers, respectively; 4,4′-bis(carbazol-9-yl)-biphenyl (CBP) and 1,3,5-tris(*N*-4-phenylbenzimidazol-2-yl)-benzene (TPBi) act as hole- and electron-transport layers, respectively; the BN-heterocycles were doped into CBP as the emissive layer. The vacuum-deposition temperature was 105 °C and 208 °C for **A1** and

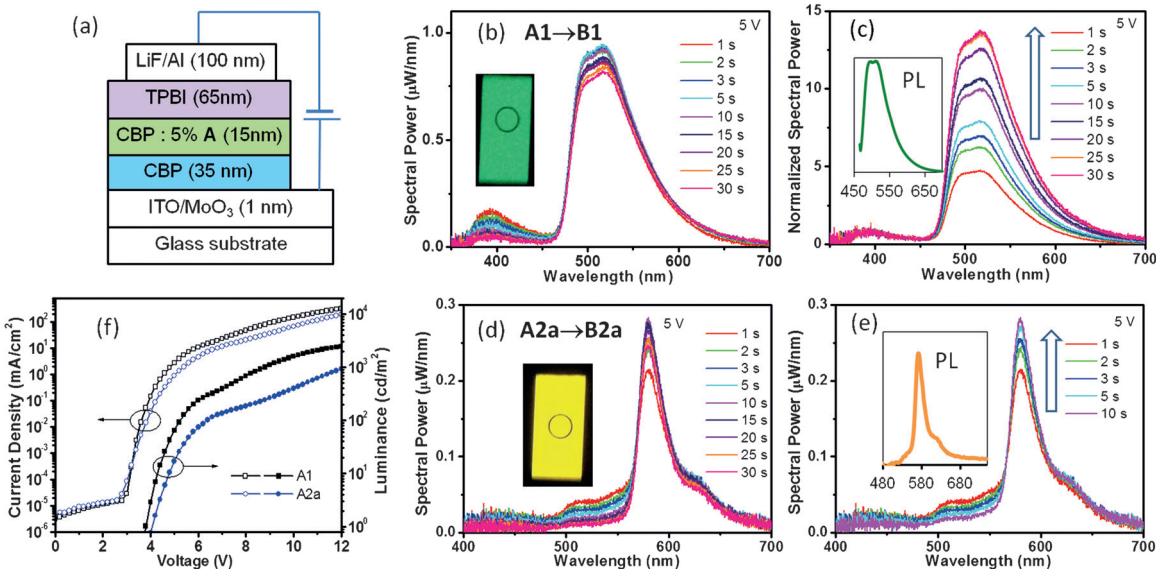

Figure 4. a) The structure of the EL device used for investigating the EDE process. b) EL spectra (spectral power versus wavelength) of the **A1**→**B1** device. c) Normalized EL spectra of the **A1**→**B1** device. d) The EL spectra of the **A2a**→**B2a** device. e) The EL spectral change of the **A2a**→**B2a** device during the first 10 s drive. Both devices were operated at a constant driving voltage of 5 V for 30 s. Each spectrum was recorded under 1 s of the constant driving voltage by taking the average of three scans with 0.3 s integration time. Insets: PL spectra of **B1** and **B2a** films, and photographs showing the emission colors of the in situ fabricated EL devices. f) The current density–luminance–voltage diagrams for **A1**- and **A2a**-based devices.

A2a, respectively, temperatures far below their melting points (218 °C for **A1**)[8] and thermal decomposition temperatures (> 280 °C for both **A1** and **A2a**,). It is important to note that the processability of the BN-heterocycles is one major advantage of our in situ strategy, as their BN-arene counterparts tend to possess poorer solubility and stability, which complicates their incorporation into optoelectronic devices and diminishes their potential value as organic materials.

To monitor the elimination process of **A1** or **A2a** driven by excitons in the EL devices, the EL spectral power versus time was recorded for the device at a constant driving voltage of 5 V (Figure 4b,c). The EL peaks, at roughly 498 and 518 nm, from the **A1**-based device match the PL spectrum of **B1**, indicating that the mesitylene elimination from **A1** can indeed be driven by excitons in EL devices. Assuming that the emission intensity of the CBP host at 392 nm is constant, the EDE process can be tracked by monitoring the emission intensity of the main peak. As shown in Figure 4b, the emission intensity of the peaks at 498 and 518 nm quickly rises to the maximum within the first 25 s of applied driving voltage, suggesting that the EDE process of **A1** to **B1** in an EL device occurs on a timescale of a few seconds under electrical bias. Based on these observations, the rate of the EDE process is estimated to be at least five orders of magnitude faster than the photoelimination process, which generally takes several hours of UV exposure for doped PMMA films.[8a] This extremely quick and efficient conversion of the BN-heterocyclic precursor to its BN-phenanthrene within the EL device is surprising; it is also the first example of a desirable chemical transformation proceeding within a normal EL device under standard operating conditions. The elimination reaction within the EL device likely proceeds through an excited-state pathway similar to photoelimination discussed in other publications,[8] where the electronic transitions to the relevant excited states of the BN-heterocycle are facilitated by the efficient and highly localized exciton generation within the device.

The **A2a**-based device also displayed fast conversion to the BN-pyrene compound **B2a** at a constant driving voltage of 5 V, with the EL intensity reaching its maximum within about 10 s (Figure 4d,e). The **A2a**-based device has a distinct yellow EL peak at 575 nm, which matches the photoluminescence properties of **B2a**. This finding indicates that the double-elimination reaction can also be effectively driven to completion using electrically generated excitons. The weak EL peak at about 520 nm which decreases in intensity with driving time may be from the single-elimination product **B2a′**. The rapid conversion of **A2a** to **B2a** in the EL device is truly remarkable, particularly given the fact that the double photoelimination of **A2a** is even slower and less efficient than the single photoelimination of **A1**. The turn-on voltages for the **A1**- and **A2a**-based devices are 3.8 and 4.2 V, respectively. Both devices demonstrate modest brightness (Figure 4f) and current efficiencies (max. $\approx$ 2.4 cd A^{-1}, and 1.9 cd A^{-1} for **A1** and **A2a**, respectively, see Figure S8), which is mainly a result of the modest photoluminescence quantum efficiency of **B1** and **B2a** (0.27). Despite its low volatility (b.p. 165 °C), the eliminated mesitylene could diffuse rapidly to the hole- and electron-transport layers with an overall concentration of about 0.5 %; however, because of its very large HOMO–LUMO gap it is unlikely to trap charges or excitons and thus has little to no influence on the EL device performance.

Compounds **A1a** and **A1b** were also found to undergo rapid EDE, producing the corresponding BN-phenanthrenes[8] and their green EL devices, in analogy to the reactions of **A1** (see Figure S8b–i). EDE in an EL device does not work well for BN-heterocycles that have alkyl substituents on the B atom such as 1,5-cyclooctyl (**A1c**, see Figure S8j)[8c] and the $B(CH_3)_2$ analogue (m.p. 120 °C)[8a] due to the low phase-transition temperature of the precursors and products.

In summary, new BN-pyrene derivatives have been achieved via a double mesitylene-elimination reaction. Furthermore, we have established that the photoelimination reaction can be extended to/and efficiently driven for several representative members of BN-heterocycles in situ through the unprecedented EDE within an EL device. The discovery of the EDE phenomenon has a number of important synthetic and practical implications, as it provides a new approach for the design and preparation of novel organic materials as well as their implementation within optoelectronic device architectures. We envision that this strategy will be most valuable for the in situ conversion/processing of stable, soluble, and readily accessible poly-BN-heterocyclic systems with high thermal stability to less stable, less soluble, and not directly accessible but highly functional poly-BN-aromatic hydrocarbons for OFETs or OLEDs. We are currently investigating the scope and applications of this unusual phenomenon.

Acknowledgements

S.W., D.-T.Y., J.S.L., X.W., S.K.M., S.G., and Z.H.L. thank the Natural Sciences and Engineering Research Council of Canada and Natural Science Foundation of China for financial support. H.S. and A.W. acknowledge the JSPS for financial support. S.W. also thanks the Beijing Institute of Technology for financial support. Synchrotron single-crystal X-ray analysis was carried out at the SPring-8 beam line BL38B1 with the approval of JASRI (2014B1556). We thank Julian Radtke for the German translation of this Communication.

Keywords: BN-heterocycles · BN-pyrenes · exciton-driven elimination · organic light-emitting diodes · solid-state reactions

How to cite: *Angew. Chem. Int. Ed.* **2015**, *54*, 15074–15078
Angew. Chem. **2015**, *127*, 15289–15293

[1] a) Z. Liu, T. B. Marder, *Angew. Chem. Int. Ed.* **2008**, *47*, 242; *Angew. Chem.* **2008**, *120*, 248; b) M. J. D. Bosdet, W. E. Piers, *Can. J. Chem.* **2009**, *87*, 8; c) P. G. Campbell, A. J. V. Marwitz, S.-Y. Liu, *Angew. Chem. Int. Ed.* **2012**, *51*, 6074; *Angew. Chem.* **2012**, *124*, 6178; d) X.-Y. Wang, J.-Y. Wang, J. Pei, *Chem. Eur. J.* **2015**, *21*, 3528.

[2] a) M. J. S. Dewar, *Tetrahedron* **1959**, *7*, 213; b) M. J. S. Dewar, R. Dietz, *J. Chem. Soc.* **1959**, 2728; c) M. J. S. Dewar, P. A. Marr, *J. Am. Chem. Soc.* **1962**, *84*, 3782; d) D. G. White, *J. Am. Chem. Soc.* **1963**, *85*, 3634; e) M. J. S. Dewar, W. H. Poesche, *J. Org. Chem.* **1964**, *29*, 1757.

[3] a) A. J. Ashe, X. D. Fang, *Org. Lett.* **2000**, *2*, 2089; b) D. J. H. Emslie, W. E. Piers, M. Parvez, *Angew. Chem. Int. Ed.* **2003**, *42*, 1252; *Angew. Chem.* **2003**, *115*, 1290; c) T. Agou, J. Kobayashi, T. Kawashima, *Chem. Commun.* **2007**, 3204; d) M. Lepeltier, O. Lukoyanova, A. Jacobson, S. Jeeva, D. F. Perepichka, *Chem. Commun.* **2010**, *46*, 7007; e) H. Braunschweig, A. Damme, O. C. Jimenez-Halla, B. Pfaffinger, K. Radacki, J. Wolf, *Angew. Chem. Int. Ed.* **2012**, *51*, 10034; *Angew. Chem.* **2012**, *124*, 10177; f) S. Xu, L. N. Zakharov, S. Y. Liu, *J. Am. Chem. Soc.* **2011**, *133*, 20152; g) V. M. Hertz, M. Bolte, H.-W. Lerner, M. Wagner, *Angew. Chem. Int. Ed.* **2015**, *54*, 8800; *Angew. Chem.* **2015**, *127*, 8924.

[4] a) C. Ma, J. Zhang, J. Li, C. Cui, *Chem. Commun.* **2015**, *51*, 5732; b) X. Liu, P. Wu, J. Li, C. Cui, *J. Org. Chem.* **2015**, *80*, 3737; c) X.-Y. Wang, A. Narita, X. Feng, K. Müllen, *J. Am. Chem. Soc.* **2015**, *137*, 7668.

[5] a) T. Hatakeyama, S. Hashimoto, S. Seki, M. Nakamura, *J. Am. Chem. Soc.* **2011**, *133*, 18614; b) X.-Y. Wang, H.-R. Lin, T. Lei, D.-C. Yang, F.-D. Zhuang, J.-Y. Wang, S.-C. Yuan, J. Pei, *Angew. Chem. Int. Ed.* **2013**, *52*, 3117; *Angew. Chem.* **2013**, *125*, 3199; c) X.-Y. Wang, F.-D. Zhuang, R.-B. Wang, X.-C. Wang, X.-Y. Cao, J.-Y. Wang, J. Pei, *J. Am. Chem. Soc.* **2014**, *136*, 3764; d) X.-Y. Wang, F.-D. Zhuang, X.-C. Wang, X.-Y. Cao, J.-Y. Wang, J. Pei, *Chem. Commun.* **2015**, *51*, 4368.

[6] a) M. J. D. Bosdet, W. E. Piers, T. S. Sorensen, M. Parvez, *Angew. Chem. Int. Ed.* **2007**, *46*, 4940; *Angew. Chem.* **2007**, *119*, 5028; b) C. A. Jaska, W. E. Piers, R. McDonald, M. Parvez, *J. Org. Chem.* **2007**, *72*, 5234.

[7] S. S. Chissick, M. J. S. Dewar, P. W. Maitlis, *Tetrahedron Lett.* **1960**, *23*, 8.

[8] a) J. S. Lu, S. B. Ko, N. R. Walters, Y. Kang, F. Sauriol, S. Wang, *Angew. Chem. Int. Ed.* **2013**, *52*, 4544; *Angew. Chem.* **2013**, *125*, 4642; b) S.-B. Ko, J.-S. Lu, S. Wang, *Org. Lett.* **2014**, *16*, 616; c) D.-T. Yang, S. M. Mellerup, X. Wang, J.-S. Lu, S. Wang, *Angew. Chem. Int. Ed.* **2015**, *54*, 5498; *Angew. Chem.* **2015**, *127*, 5588.

[9] N. J. Turro, V. Ramamurthy, J. C. Scaiano, *Principles of Molecular Photochemistry*: *An Introduction*, University Science Books, Sausalito, **2009**.

[10] L.-Y. Liao, X.-R. Kong, X.-F. Duan, *J. Org. Chem.* **2014**, *79*, 777.

[11] T. Sajoto, P. I. Djurovich, A. B. Tamayo, J. Oxgaard, W. A. Goddard III, M. E. Thompson, *J. Am. Chem. Soc.* **2009**, *131*, 9813.

Received: August 19, 2015
Published online: October 20, 2015

